

# Biochemistry

© Copyright 1999 by the American Chemical Society

Volume 38, Number 8

February 23, 1999

## Accelerated Publications

---

### Multiple Types of Association of Photosystem II and Its Light-Harvesting Antenna in Partially Solubilized Photosystem II Membranes

Egbert J. Boekema,<sup>‡</sup> Henny van Roon,<sup>§</sup> Florentine Calkoen,<sup>§</sup> Roberto Bassi,<sup>||</sup> and Jan P. Dekker<sup>\*,§</sup>

Department of Biophysical Chemistry, Groningen Biomolecular Sciences and Biotechnology Institute, University of Groningen, Nijenborgh 4, 9747 AG Groningen, The Netherlands, Department of Physics and Astronomy, Institute of Molecular Biological Sciences, Vrije Universiteit, De Boelelaan 1081, 1081 HV Amsterdam, The Netherlands, and Università degli Studi di Verona, Facoltà di Scienze MM. FF. e NN., Strada Le Grazie, Ca'Vignal, I-37134 Verona, Italy

Received November 13, 1998; Revised Manuscript Received December 23, 1998

**ABSTRACT:** Photosystem II is a multisubunit pigment–protein complex embedded in the thylakoid membranes of chloroplasts. It utilizes light for photochemical energy conversion, and is heavily involved in the regulation of the energy flow. We investigated the structural organization of photosystem II and its associated light-harvesting antenna by electron microscopy, multivariate statistical analysis, and classification procedures on partially solubilized photosystem II membranes from spinach. Observation by electron microscopy shortly after a mild disruption of freshly prepared membranes with the detergent *n*-dodecyl- $\alpha$ , $\beta$ -D-maltoside revealed the presence of several large supramolecular complexes. In addition to the previously reported supercomplexes [Boekema, E. J., van Roon, H., and Dekker, J. P. (1998) *FEBS Lett.* 424, 95–99], we observed complexes with the major trimeric chlorophyll *a/b* protein (LHCII) in a third, L-type of binding position ( $C_2S_2M_{0-2}L_{1-2}$ ), and two different types of megacomplexes, both identified as dimeric associations of supercomplexes with LHCII in two types of binding sites ( $C_4S_4M_{2-4}$ ). We conclude that the association of photosystem II and its associated light-harvesting antenna is intrinsically heterogeneous, and that the minor CP26 and CP24 proteins play a crucial role in the supramolecular organization of the complete photosystem. We suggest that different types of organization form the structural basis for photosystem II to specifically react to changing light and stress conditions, by providing different routes of excitation energy transfer.

The photosynthetic apparatus of green plants and algae is a highly complex system consisting of a number of multi-subunit protein complexes bound to thylakoid membranes of chloroplasts. One of these complex systems is photosystem II (PSII),<sup>1</sup> which uses light energy for the reduction of

plastoquinone, the oxidation of water, and the formation of a transmembrane pH gradient. It consists of at least 25 different types of protein subunits (*I*), many of which are bound to the thylakoid membrane. Some subunits are involved in the capturing of solar energy and the regulation

---

\* To whom correspondence should be addressed. Telephone: +31 20 4447931. Fax: +31 20 4447999. E-mail: dekker@nat.vu.nl.

<sup>‡</sup> University of Groningen.

<sup>§</sup> Vrije Universiteit Amsterdam.

<sup>||</sup> Università degli Studi di Verona.

<sup>1</sup> Abbreviations:  $\alpha$ -DM, *n*-dodecyl- $\alpha$ , $\beta$ -D-maltoside; C, photosystem II core complex; Chl, chlorophyll; L, loosely bound trimeric LHCII; LHCII, light-harvesting complex II; M, moderately bound trimeric LHCII; PSI, photosystem I; PSII, photosystem II; qE, nonphotochemical quenching; S, strongly bound trimeric LHCII; X, extra loosely bound trimeric LHCII.

of the energy flow; others are directly or indirectly responsible for the photochemistry, including the oxidation of water to molecular oxygen.

The central part of the complete PSII unit is formed by the so-called core complex, a well-defined structure of which the reaction center proteins D1 and D2 and the core antenna proteins CP47 and CP43 are the largest and functionally the most important components (1). This structure is responsible for all electron-transfer reactions in PSII, including the formation of oxygen. There is overwhelming evidence that the PSII core complex is organized as a dimer in the stacked, appressed regions of the thylakoid membrane (see, e.g., 2, 1). The projected structure of the PSII core complex without the CP43 subunit has been determined at 8 Å resolution by electron crystallography on two-dimensional crystals (3), and three-dimensional maps at lower resolution have also been reported (see, e.g., 4).

The dimeric PSII core complex is surrounded by the peripheral antenna, which in green plants and algae consists of an unknown structure of several light-harvesting complex II (LHCII) proteins that together bind a large number of chlorophyll *a*, chlorophyll *b*, and carotenoid (xanthophyll) molecules. The LHCII proteins are encoded by the sequence-related nuclear genes designated *Lhcb1–6*. *Lhcb1* and *Lhcb2* encode the two most abundant proteins in the thylakoid membrane, which together with the minor *Lhcb3* protein form the major trimeric LHCII complex (5, 6). The three other proteins *Lhcb4* (CP29), *Lhcb5* (CP26) and *Lhcb6* (CP24) are monomeric and probably more closely associated with the PSII core complex than the *Lhcb1–3* gene products (5, 6). The structure of the major trimeric LHCII complex is known at 3.4 Å resolution (7, 8). All *Lhcb* gene products show strong sequence homology, in particular in the transmembrane  $\alpha$ -helices.

Despite the impressive progress on the knowledge of the structure and organization of most of the PSII proteins, it is still not known how the various proteins in the thylakoid membranes cooperate to convert the light energy so efficiently. A basic understanding of the organization of thylakoid membranes *in vivo* has been obtained from freeze-etch and freeze-fracture electron microscopy, which give images with structural detail at 40–50 Å resolution (9). Considerably more detail, however, is required to understand the role of the various proteins in the energy flow to the reaction center and in the dynamics related to short-term acclimation processes (6, 10). The isolation of a PSII dimer surrounded by two copies of CP29, CP26, and trimeric LHCII (11) and the characterization of this complex by electron microscopy and image analysis (12) revealed first details of the structural organization of the PSII core and part of its associated antenna. We will abbreviate this complex as  $C_2S_2$  in the present paper, in which “C” refers to a monomeric PSII core complex and “S” to a “strongly” bound trimeric LHCII. Cross-linking studies on an even larger supercomplex suggested the locations of the CP29 and CP26 proteins, while also locations for CP24 and another trimeric LHCII were proposed (13).

Recently, we started to investigate the supramolecular organization of PSII and its associated antenna by electron microscopy and image analysis on partially solubilized grana membranes (14). The time of exposure to detergent was kept to a minimum (<5 min) to prevent fragmentation of the

fragile supramolecular complexes as much as possible and to avoid the risk of artificial aggregation due to extensive biochemical manipulation (15). The results revealed the presence of larger supercomplexes ( $C_2S_2M_{1-2}$ ) with “moderately” bound trimeric LHCII (“M”) and a monomeric protein on exactly the same position as independently proposed by Harrer et al. (13) on the basis of their cross-linking studies.

In this report, we present a much more elaborate analysis of the partially solubilized PSII membranes. To facilitate the EM analysis, we partially purified the solubilized fractions by gel filtration chromatography. From a data set of 10 600 projections, we found new characteristic associations of PSII and its light-harvesting antenna, including a number of supercomplexes with LHCII in a third type of binding position (“L”, indicating “loosely” bound LHCII) and two different types of mega-complexes ( $C_4S_4M_{2-4}$ ). We propose that the various types of association form the structural basis of PSII to respond to short-term changes of the quality and quantity of the excitation light.

## MATERIALS AND METHODS

*Sample Preparation and Biochemical Characterization.* PSII membranes were isolated from freshly prepared spinach thylakoid membranes as described before (16), except that after the second precipitation step the pellet with the PSII membranes was resuspended in a buffer containing 20 mM BisTris (pH 6.5) and 5 mM  $MgCl_2$ , and that the PSII membranes were not frozen until use. The PSII membranes were diluted in 20 mM BisTris (pH 6.5), 5 mM  $MgCl_2$ , and *n*-dodecyl- $\alpha$ ,D-maltoside ( $\alpha$ -DM, Sigma) at 4 °C to reach final concentrations of 1.9 mg of Chl/mL and 1.2%  $\alpha$ -DM. The suspension was stirred for 5 s, centrifuged for 3 min at 9000 rpm in an Eppendorf 5414 table centrifuge, and pushed through a 0.45  $\mu$ m filter to remove unsolubilized material. The solubilized material was subjected to gel filtration chromatography, using a Superdex 200 HR 10/30 column (Pharmacia) as described before (17), but with 20 mM BisTris (pH 6.5) and 0.03%  $\alpha$ -DM as mobile phase. The fractions eluting at 0.4–1.0 min after the highest absorption of the first main peak contained the largest amount of supercomplexes and were prepared for electron microscopy immediately after elution. The investigated fractions were characterized by an  $A_{470}/A_{435}$  ratio of 0.60–0.62 (14). The minor proteins CP29, CP26, and CP24 were isolated and purified from Tris-washed PSII membranes from spinach by using isoelectric focusing and sucrose density gradient centrifugation as in ref 18.

*Biochemical Characterization.* The isolated fractions were characterized by means of their absorption spectrum, isoelectric point, and polypeptide pattern. SDS-PAGE was performed using the system developed by Schägger and von Jagow (19).

*Electron Microscopy.* For electron microscopy, the sample was diluted 6-fold in 10 mM BisTris (pH 6.5) + 0.015%  $\alpha$ -DM, and prepared using the droplet method with 2% uranyl acetate as the negative stain on glow-discharged carbon-coated copper grids. During the staining procedure, the grid was washed once with distilled water to reduce detergent aggregation in the background. Electron microscopy was performed with a Philips CM10 electron micro-

scope using 100 kV at 52000 $\times$  magnification. Micrographs were digitized with a Kodak Eikonix Model 1412 CCD camera with a scan step of 25  $\mu$ m, corresponding to a pixel size of 4.85  $\text{\AA}$ .

**Image Analysis.** From 107 images, all well-preserved top-view projections with the size of a supercomplex, or larger, were extracted. The 7300 selected projections were aligned, treated by multivariate statistical analysis, and classified with IMAGIC software as described previously (20, 12). In an initial classification, the data set was decomposed in 100 classes, which appeared to represent 5 rather homogeneous groups of different types of projections and about 20% misaligned projections. Next, the aligned parts of the 7300 projections were divided into 5 subsets consisting of the above-mentioned groups. For the 4 less numerous subsets, the similar projections of the previous data set of 3300 projections (14) were added. The five subsets were separately processed and classified. Their analysis resulted in the finding of two additional types of projections. Finally, classes from each of the subsets were used for refinement of alignments and subsequent classifications, and searches for interpretable views were performed among projections misaligned in the initial classification step. The resolution of the images was measured by comparing the two half-images by Fourier correlation (21).

## RESULTS

**Sample Preparation.** To analyze large associations of PSII and its light-harvesting antenna, we added the relatively mild nonionic detergent *n*-dodecyl- $\alpha$ , $\beta$ -D-maltoside ( $\alpha$ -DM) to freshly prepared PSII membranes. To make sure that the amount of detergent is the limiting factor in the solubilization process, we added an about 2-fold smaller amount of detergent than required to completely solubilize these membranes. It is therefore likely that almost all detergent molecules will be attached to the hydrophobic surfaces of the membrane proteins under these conditions, thus minimizing further disintegration of the various associations by free detergent molecules, and that most of the inner shell of lipids will remain bound to the complexes. We checked that the pigment and protein compositions of the solubilized and nonsolubilized fractions were similar (by absorption spectra and SDS-PAGE, respectively), which suggests that a random fraction of the PSII membranes was solubilized.

This strategy was also applied in our previous report (14), where we analyzed the complete set of solubilized proteins by electron microscopy. However, the image analysis was hampered to some extent because of the large amount of relatively small fragments, which predominantly consist of trimeric LHCII. We therefore partially purified the solubilized fractions by gel filtration chromatography. The increase of the time of detergent exposure from a few minutes to up to 1 h appeared not to have significant effects on the composition of the solubilized associations. SDS-PAGE showed that the investigated fractions contained all major and minor LHCII proteins (Figure 1). In particular, our material contains the minor protein CP24, which was reported to be absent in the original  $C_2S_2$  supercomplex (11) but present in a larger association (13).

**Image Analysis.** Inspection of electron micrographs from chromatography-purified PSII membranes showed the pres-

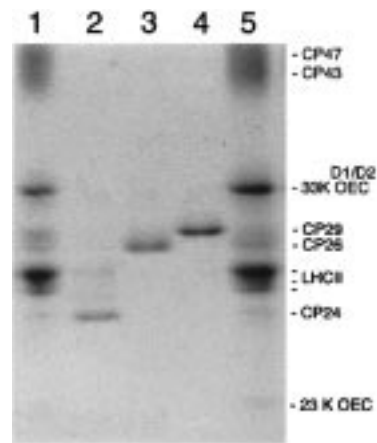


FIGURE 1: Identification of polypeptides in chromatography-purified, partially  $\alpha$ -DM-solubilized PSII membranes by SDS-PAGE. Lane 1, fraction eluting at 0.4 min after the highest absorption of the first main peak in the chromatogram [see Materials and Methods and (14)]. Lane 2, fractions containing  $\sim$ 75% purified CP24. Lane 3, fraction containing  $\sim$ 95% purified CP26. Lane 4, fraction containing  $\sim$ 95% purified CP29. Lane 5, fraction eluting at 0.8 min after the highest absorption of the first main peak in the chromatogram. The gel was stained with Coomassie Brilliant Blue. "33K OEC" and "23K OEC" refer to extrinsic proteins involved in oxygen evolution with apparent molecular masses of 33 and 23 kDa, respectively.

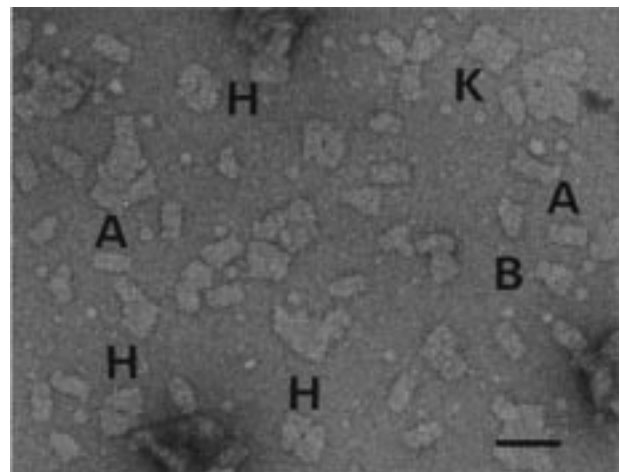


FIGURE 2: Part of an electron micrograph showing various types of PSII-LHCII complexes isolated from partially solubilized PSII membranes and negatively stained with 2% uranyl acetate. Some of the mega- and supercomplexes have been marked with letters that correspond to the average images of these projections presented in Figure 3. Bar represents 500  $\text{\AA}$ .

ence of many large top-view projections (Figure 2). Small fragments of the size of trimeric LHCII and "sandwiches" of two appressed PSII complexes were relatively scarce. The top-view projections appear with a strong preference for one type of handedness (the "flip" projection), a feature that was also noted for other PSII preparations (22, 23). The most abundant complex was a 2-fold symmetrical supercomplex ("A" in Figure 2), consisting of a dimeric PSII core complex surrounded by two trimeric LHCII complexes, named  $C_2S_2$  in the short nomenclature introduced previously (14). Other complexes, with an LHCII trimer in the M-position ( $C_2S_2M$ ), were also visible (marked "B" in Figure 2). Besides these previously characterized types of projections, several new types of projections were present (e.g., those marked "H" and "K" in Figure 2).

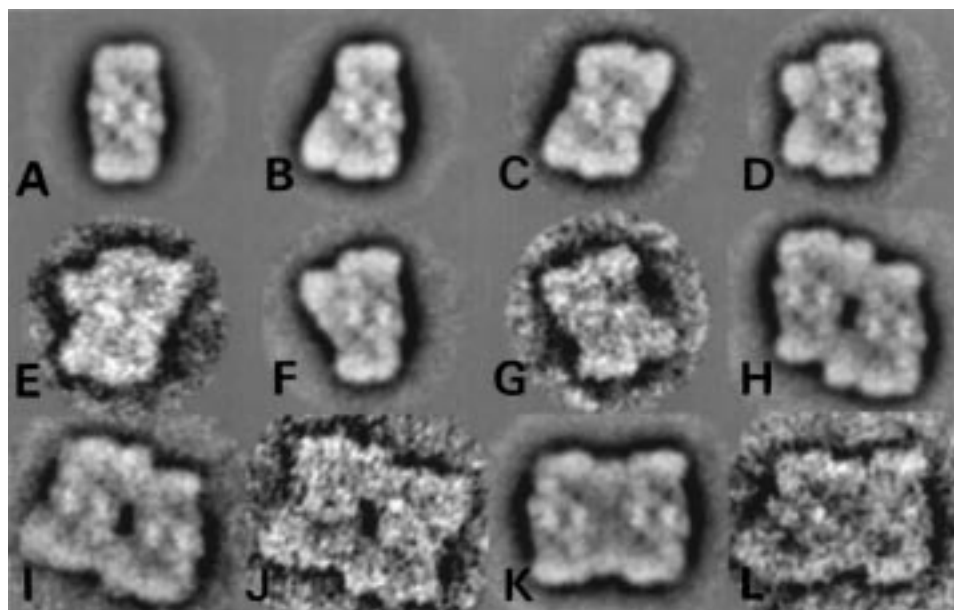


FIGURE 3: Average projections of (A) the best 600  $C_2S_2$ , (B) the best 360  $C_2S_2M$ , (C) 91  $C_2S_2M_2$ , (D) 86  $C_2S_2ML$ , (E) 6  $C_2S_2M_2L$ , (F) 65  $C_2S_2L$ , and (G) 6  $C_2S_2L_2$  supercomplexes, and (H) 115 type I  $C_4S_4M_2$ , (I) 25 type I  $C_4S_4M_3$ , (J) 3 type I  $C_4S_4M_4$ , (K) 150 type II  $C_4S_4M_2$  and (L) 6 type II  $C_4S_4M_3$  megacomplexes, found by classification of a data set of 10 600 projections. Note: No rotational symmetry was imposed on the images.

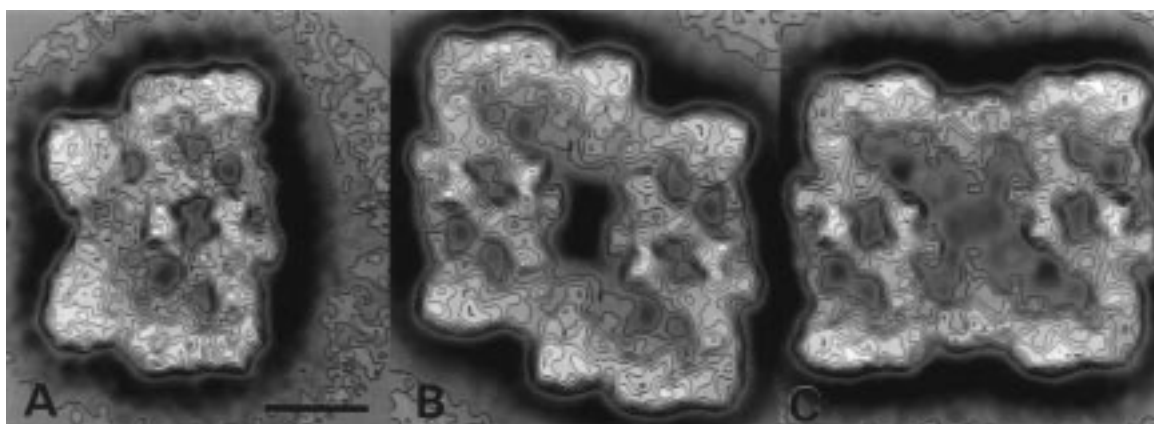


FIGURE 4: Contoured versions of the most detailed sums of supercomplexes and megacomplexes. (A) The  $C_2S_2ML$  supercomplex presented in Figure 3D. (B) The type I  $C_4S_4M_2$  megacomplex presented in Figure 3H. (C) The type II  $C_4S_4M_2$  megacomplex presented in Figure 3K. Notes: On images B and C, 2-fold rotational symmetry was imposed; scale bar = 100 Å.

To investigate the structural variation among the various PSII–LHCII projections, we focused in this investigation only on the complexes larger than  $C_2S_2$ . To study all projections in a computer-economic way, we split the data set after initial classification into five subsets of similar types of projections, belonging to the groups  $C_2S_2$ ,  $C_2S_2M$ ,  $C_2S_2M_2$ ,  $C_2S_2ML$ , and  $C_4S_4M_2$ , respectively. The analysis of the latter two subsets is described below; the analysis of the first three subsets partially overlaps with our earlier work (14), and will be further described in detail elsewhere (see Figure 3A–C for final results of the  $C_2S_2$ ,  $C_2S_2M$ , and  $C_2S_2M_2$  projections, respectively) together with a study on the rotational orientation of LHCII.

*Analysis of  $C_2S_2ML$ ,  $C_2S_2L$ , and  $C_2S_2L_2$  Supercomplexes.* In the present data set, a new (fourth) subset is observed with a type of projection like  $C_2S_2M$  (Figure 3B), but with additional mass in the upper left part of the complex. Classification of 125 projections gave a sharply outlined sum of 85 projections, from which it becomes clear that the extra mass has the size of a trimeric LHCII protein (Figure 3D).

Since only a small number (7%) of the  $C_2S_2M$  supercomplexes have this extra mass, it is defined as “L” (from “loose”) in our nomenclature, and the supercomplex is called  $C_2S_2ML$  (see Figure 4A for a contoured version).

This finding prompted us to look if the L-part would also be present in other types of complexes. In the subset of the  $C_2S_2M$  type of particles, 2 classes comprising 225 projections consisted mainly of projections with the other handedness, the so-called “flop” projections (not shown). Since a potential  $C_2S_2L$  projection has some similarities with the flop-type projection of  $C_2S_2M$ , this data set was further classified. This resulted in the finding that about one-third of these projections were not  $C_2S_2M$  flop-projections, but indeed belong to a projection type that can be described as  $C_2S_2L$  (Figure 3F). Searching for the symmetrical  $C_2S_2L_2$  supercomplex revealed a few projections of this type (Figure 3G).

The finding of another LHCII trimer in an alternative third binding position implies that if all three LHCII binding positions would be occupied, six LHCII trimers should surround a dimeric supercomplex. However, a systematic

search resulted in finding only six particles with five LHCII trimers (Figure 3E) and none with six trimers. Statistically seen, this is not a total surprise, in light of the ratio of  $C_2S_2M$  to  $C_2S_2M_2$  and  $C_2S_2L$  to  $C_2S_2L_2$  (both about 10:1) and of the ratio of  $C_2S_2M$  to  $C_2S_2ML$  (about 15:1). However, in a data set of 10 600 one might expect to find some, even if such complexes are prone to fractionation by the detergent. The fact that such a particle has not been observed leads us to conclude that the supercomplex with six LHCII trimers is also rare because the “L” component is not present in stoichiometric quantities. The finding of “megacomplexes” supports this conclusion (see below).

*Analysis of Megacomplexes.* The fifth and last subset consisted of about 600 projections with a square-like shape and a size of at least 2  $C_2S_2$  supercomplexes. By further classification, we found that this subset was inhomogeneous, but in a specific way. It consisted not only of square-like projections (Figure 3H), but also of rather rectangular-shaped projections (Figure 3K). In the following, the two types are denoted as “megacomplex type I” and “megacomplex type II”, respectively. The term “megacomplex” refers to the about double size compared to the various supercomplexes (Figure 3A–G). In our preparations, the square-like type I was about 3 times more abundant. The type I megacomplex is easily recognizable by its stain-filled central cavity, which is very strong in most projections. Both types of megacomplexes appear to be built up from two perfectly parallel-arranged  $C_2S_2$  supercomplexes (tests: within  $0.5^\circ$ ), with additional mass in between. The parallel arrangement strongly suggests the presence of a 2-fold symmetry axis. A closer inspection reveals that both megacomplexes consist of two  $C_2S_2M$  types of supercomplexes and that the two  $C_2S_2M$  halves are  $180^\circ$  rotated. Type II has the same constitution as type I, but with the two halves translationally shifted toward each other. Upon 2-fold averaging, these details become enhanced (Figure 4B–C). The classification further showed variation in a similar way as seen in the supercomplexes. The basic  $C_4S_4M_2$  unit can also be larger ( $C_4S_4M_3$ , Figure 3I,L; or  $C_4S_4M_4$ , Figure 3J). We even noticed one type II projection of the  $C_4S_4M_4L_2$  type (not shown).

## DISCUSSION

*Do the Observed Complexes Represent in Vivo Organizations?* In this report, we present several new types of association of PSII and LHCII. It can be estimated that the megacomplexes shown in Figure 4B,C have a molecular mass of about 1600 kDa, which means that they represent the largest isolated associations of PSII and LHCII that have been observed thus far.

An important issue regarding these new findings is the question whether the observed megacomplexes and larger supercomplexes can be considered to be present in the thylakoid membrane in vivo and do not form after membrane disruption. There are several arguments against potential formation during or after isolation:

(a) In the data set of 3300 nonpurified particles selected from specimens fixed within minutes after the partial disruption of grana membranes by a mild detergent (14), all major types of larger associations appear to be present (e.g., those shown in Figure 4A–C), though in low numbers. This means that artificial aggregates, if any, must have occurred in a very short time.

(b) The relative occurrence of megacomplexes and larger supercomplexes in this report and in our previous report (14) is similar, despite an initial (before chromatography) about 20-fold difference in protein and detergent concentration. If artificial aggregation would occur, it would be more prominent at higher protein concentrations.

(c) Some type I megacomplex particles are visible in irregularly shaped membrane fragments of over 2 times their own sizes. In such fragments, these megacomplexes are easily recognizable from the characteristic stain-filled central density and jagged edges (not shown).

(d) Particles that have been shown to be artificial aggregations (15) require an intermediate aggregation/disaggregation step. In our particles, the detergent concentration was always kept above the critical micelle concentration. In addition, freezing/thawing procedures, which in principle also could give rise to artificial associations, were completely avoided.

It is furthermore worthwhile to note that the resolution of the larger complexes (18–22 Å, Figure 4A–C) is not substantially lower than that of the ‘standard’ supercomplexes  $C_2S_2$  and  $C_2S_2M$  (14). This means that the way of association of the L-type of LHCII and of the megacomplexes must be very specific. If considerable disorder would occur in the binding of the various units, the resolution of the complexes would be lower.

*Supramolecular Organization of PSII in Grana Membranes.* At present, we do not have indications for PSII–LHCII complexes with more than three types of binding sites. Nevertheless, on the basis of biochemical considerations, about four trimeric LHCII complexes are thought to be present on every monomeric PSII unit (see, e.g., 24, 5, 11), suggesting that every dimeric PSII core complex could be surrounded by eight trimeric LHCII complexes and that there may be four different types of LHCII binding sites. It is possible that a very loose association of, for instance, the  $C_2S_2ML$  particle with a fourth type of LHCII (“X”, from “extra loose”) is overlooked. However, a search for an X-type of LHCII at the most obvious position (on top of the L-type of LHCII in Figure 4A) had a negative result.

We can only speculate on the relation between LHCII in the various binding sites (S, M, and L), the X-LHCII that is not observed in our work, and the ‘tightly bound’ and ‘mobile’ populations of LHCII discussed previously (25, 26). It is possible that the ‘tightly bound’ population includes S, M, and perhaps even L, and that the ‘mobile’ population only involves the LHCII that is not directly associated with PSII.

An interesting point is the simultaneous occurrence of supercomplexes with at least one occupied L-type of binding site (Figure 3D–G) and of megacomplexes, which cannot have an occupied L-type of binding site between the two supercomplexes (Figure 3H–L). This shows that the association of the PSII core and LHCII is intrinsically heterogeneous. These results extend the large number of freeze–etching studies, which have shown that in the stacked thylakoid membrane PSII core complexes (and their unresolved antenna system) are usually randomly positioned (9). Only in some special cases, ordered two-dimensional lattices have been shown to occur. The lattice dimensions of such arrays are quite variable, but usually much smaller than expected for PSII dimers surrounded by four trimeric LHCII proteins (with  $C_2S_2M_2$  as basic unit) or by six trimeric LHCII

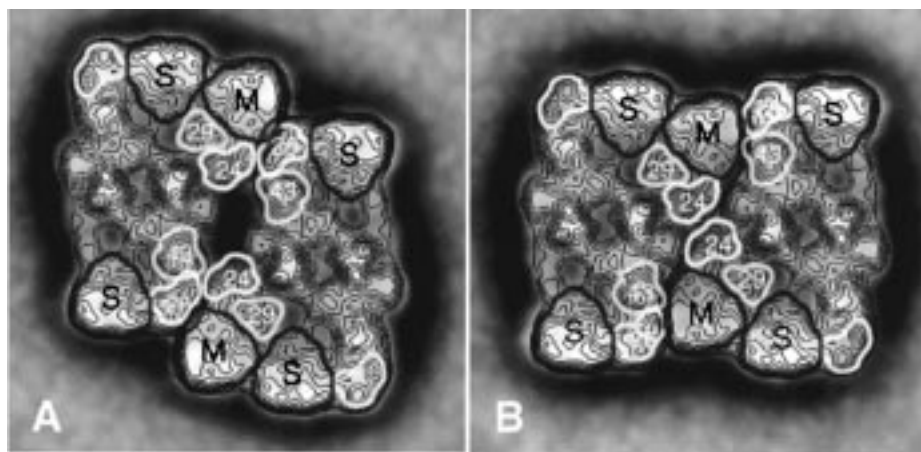


FIGURE 5: Scheme showing subunit interactions in the type I (A) and type II (B) megacomplexes of PSII and LHCII. Density contours of the  $C_2S_2M$  supercomplex have been superimposed on the images of the megacomplexes (Figure 3H,K), and antenna components have been outlined. "S" and "M" refer to trimeric LHCII in the S-type and M-type of binding position, respectively, whereas the numbers "24", "26", "29", and "43" indicate the positions of the CP24, CP26, CP29, and CP43 proteins, respectively.

proteins (with  $C_2S_2M_2L_2$  as basic unit). The larger lattices might be caused by  $C_2S_2$  supercomplexes (see, e.g., 1), the smaller ones by just PSII core complexes (27). One should keep in mind, however, that at least some of these arrays, in particular the smaller ones, are likely to be the result of the detergent treatment (see, e.g., 27), and that these arrays may not have anything to do with the physiological situation. Until now, periodic averaging of two-dimensionally ordered arrays has not shown clear details of the antenna structure, as discussed recently in ref 1.

We would like to stress that the observed large associations should be rather flexible. There is no doubt that the innermost PSII reaction centers in megacomplexes and in complexes containing the L-type LHCII are almost completely surrounded by peripheral antenna proteins (Figure 4A–C). For normal functioning, the plastoquinone electron acceptors (which due to their hydrophobicity only occur in the lipid phase of the membrane) need to have good access to the heart of the reaction center to ensure efficient electron transfer from PSII to PSI. This means that the antenna proteins must provide some channel for plastoquinone or must at least be so flexible that there are no severe restrictions to reach the photochemical reaction center. Furthermore, the antenna system should also allow the exchange of the D1 protein under photoinhibitory conditions, which seems unlikely in case of a very rigid organization.

*Role of CP29, CP26, and CP24 in the Supramolecular Organization of PSII.* One of the most important results of our work is that there are at least three principally different ways by which PSII and LHCII interact. All associations have in common that they bind LHCII at S- and M-positions around a dimeric PSII core complex. Thus, the  $C_2S_2M_2$  unit could be viewed as the basic building block of the various larger associations. This complex can then form either a type I association (as in the type I megacomplex), a type II association (as in the type II megacomplex), or an association with additional LHCII at the L-position.

The resolution of our images permits us to give details on the contact sites that form the basis of the three types of association. The type I megacomplex (Figure 4B) has a very open structure in which the PSII core parts of both supercomplexes make no direct contact. Actually, all contacts are

formed by two symmetrically identical interfaces, and are provided by two densities attributed to CP26 in one supercomplex and by densities of M-LHCII and CP24 in the other (Figure 5A). In the type II megacomplexes, the contacts are different. Here, a more closed structure appears with several types of contact (Figure 5B). In the binding of L-LHCII to the  $C_2S_2M_{0-2}$  supercomplex, again CP26, CP24, and the PSII core contribute. This association resembles that of the upper part of the type II association, but the L-LHCII is buried deeper in the complex to provide the contact with the CP24 of the other half of the complex.

We conclude from these considerations that the minor LHC proteins CP26 and CP24 are essential for all three types of interaction. In contrast, CP29 is not involved in these interactions, because it is shielded from the interface of the megacomplexes and from LHCII at the L-position by the CP24 protein. It is tempting to speculate that the observed structural differences between CP29 on one hand and CP26 and CP24 on the other are related to reported functional differences. First, CP29 can be phosphorylated, unlike CP26 and CP24, although its phosphorylation site (28) and physiological response (6) are different from those of trimeric LHCII. Second, CP29 has a relatively high content of violaxanthin, just like CP26 and CP24, but the deepoxidation of violaxanthin to zeaxanthin under conditions of nonphotochemical quenching seems to occur mainly in CP26 and CP24 (29, 30).

In the megacomplexes and larger supercomplexes that we observed, CP26 and CP24 play key roles. In addition, there can be differences by which the excitation energy migrates from the major antenna complexes (the trimeric LHCII proteins) to the PSII core. The L-LHCII seems to have direct contact with the CP43 and reaction center parts of the core complex, and thus is expected to provide efficient energy transfer to the reaction center. This type of LHCII could be particularly relevant for plants grown under low-light conditions, which are characterized by increased concentrations of trimeric LHCII (see, e.g., 26). Type I and II associations give rise to the same number of trimeric LHCII per PSII, but differ in the contact points. In type I, the three minor proteins seem to form a cluster in the center of the megacomplex, with CP24 in the middle. Consequently,

almost all energy transfer from the M-LHCII to PSII has to pass this cluster of minors and can be reduced if quenchers are present. Only the S-LHCII seems to have some direct contact with the PSII core. In contrast, in type II the three minor proteins do not cluster together, and a direct contact between the M-LHCII and the PSII core occurs.

We conclude that the observed differences of organization can give rise to different efficiencies by which the light energy is transferred from the major light-harvesting complexes to the photochemical reaction center and thus provide the system a way to regulate the efficiency of photosynthesis under various light or stress conditions that green plants may undergo. An analysis of complexes extracted from thylakoid membranes of plants grown under different conditions might give further clues.

#### ACKNOWLEDGMENT

We thank Mr. J. F. L. van Breemen for technical assistance, Dr. W. Keestra for help with computer image analysis, Mr. K. Gilissen for photography, and Dr. H. van Amerongen, Prof. R. van Grondelle, and Prof. A. Brisson for stimulating discussions.

#### REFERENCES

- Hankamer, B., Barber, J., and Boekema, E. J. (1997) *Annu. Rev. Plant Phys. Plant Mol. Biol.* 48, 641–672.
- Santini, C., Tidu, V., Tognon, G., Ghiretti Magaldi, A., and Bassi, R. (1994) *Eur. J. Biochem.* 221, 307–315.
- Rhee, K.-H., Morris, E. P., Zheleva, D., Hankamer, B., Kühlbrandt, W., and Barber, J. (1997) *Nature* 389, 522–526.
- Morris, E. P., Hankamer, B., Zheleva, D., Friso, G., and Barber, J. (1997) *Structure* 5, 837–850.
- Jansson, S. (1994) *Biochim. Biophys. Acta* 1184, 1–19.
- Bassi, R., Sandonà, D., and Croce, R. (1997) *Physiol. Plant.* 100, 769–779.
- Kühlbrandt, W., Wang, D. N., and Fujiyoshi, Y. (1994) *Nature* 367, 614–621.
- Kühlbrandt, W. (1994) *Curr. Opin. Struct. Biol.* 4, 519–528.
- Staehelin, L. A., and van der Staay, G. W. M. (1996) in *Oxygenic Photosynthesis: The Light Reactions* (Ort, D. R., and Yocum, C. F., Eds.) pp 11–30, Kluwer Academic Publishers, Dordrecht, The Netherlands.
- Horton, P., Ruban, A. V., and Walters, R. G. (1996) *Annu. Rev. Plant Physiol. Plant Mol. Biol.* 47, 655–684.
- Hankamer, B., Nield, J., Zheleva, D., Boekema, E., Jansson, S., and Barber, J. (1997) *Eur. J. Biochem.* 243, 422–429.
- Boekema, E. J., Hankamer, B., Bald, D., Kruij, J., Nield, J., Boonstra, A. F., Barber, J., and Rögner, M. (1995) *Proc. Natl. Acad. Sci. U.S.A.* 92, 175–179.
- Harrer, R., Bassi, R., Testi, M. G., and Schäfer, C. (1998) *Eur. J. Biochem.* 255, 196–205.
- Boekema, E. J., van Roon, H., and Dekker, J. P. (1998) *FEBS Lett.* 424, 95–99.
- Eijkelhoff, C., Dekker, J. P., and Boekema, E. J. (1997) *Biochim. Biophys. Acta* 1321, 10–20.
- Berthold, D. A., Babcock, G. T., and Yocum, C. F. (1981) *FEBS Lett.* 134, 231–234.
- Eijkelhoff, C., van Roon, H., Groot, M.-L., van Grondelle, R., and Dekker, J. P. (1996) *Biochemistry* 35, 12864–12872.
- Dainese, P., Hoyer-Hansen, G., and Bassi, R. (1990) *Photochem. Photobiol.* 51, 693–703.
- Schägger, H., and von Jagow, G. (1987) *Anal. Biochem.* 166, 368–379.
- Harauz, G., Boekema, E., and van Heel, M. (1988) *Methods Enzymol.* 164, 35–49.
- Van Heel, M. (1987) *Ultramicroscopy* 21, 95–100.
- Boekema, E. J., and Rögner, M. (1996) in *Biophysical Techniques in Photosynthesis* (Amesz, J., and Hoff, A. J., Eds.) pp 325–336, Kluwer Academic Publishers, Dordrecht, The Netherlands.
- Boekema, E. J., Nield, J., Hankamer, B., and Barber, J. (1998) *Eur. J. Biochem.* 252, 268–276.
- Peter, G. F., and Thornber, J. P. (1991) *J. Biol. Chem.* 266, 16745–16754.
- Spangfort, M., and Andersson, B. (1989) *Biochim. Biophys. Acta* 977, 163–170.
- Melis, A. (1996) in *Oxygenic Photosynthesis: The Light Reactions* (Ort, D. R., and Yocum, C. F., Eds.) pp 523–538, Kluwer Academic Publishers, Dordrecht, The Netherlands.
- Lyon, M. K. (1998) *Biochim. Biophys. Acta* 1364, 403–419.
- Testi, M. G., Croce, R., Polverino de Laureto, P., and Bassi, R. (1996) *FEBS Lett.* 399, 245–250.
- Ruban, A. V., Young, A. J., Pascal, A. A., and Horton, P. (1994) *Plant Physiol.* 104, 227–234.
- Croce, R., Breton, J., and Bassi, R. (1996) *Biochemistry* 35, 11142–11148.

BI9827161